Title

Functional Differences between IgM and IgD Signaling in Chronic Lymphocytic Leukemia

Journal

The Journal of Immunology, 197(6)

ISSN

0022-1767

Authors

Ten Hacken, Elisa

Sivina, Mariela

Kim, Ekaterina

et al.

Publication Date

2016-09-15

DOI

10.4049/jimmunol.1600915

Published in final edited form as:

J Immunol. 2016 September 15; 197(6): 2522–2531. doi:10.4049/jimmunol.1600915.

Functional Differences Between IgM and IgD Signaling in Chronic Lymphocytic Leukemia

Elisa ten Hacken[*], **Mariela Sivina**[*], **Ekaterina Kim**[*], **Susan O'Brien**[*], **William G. Wierda**[*], **Alessandra Ferrajoli**[*], **Zeev Estrov**[*], **Michael J. Keating**[*], **Thomas Oellerich**[†], **Cristina Scielzo**[‡], **Paolo Ghia**[‡], **Federico Caligaris-Cappio**[‡], and **Jan A. Burger**[*]

[*]Department of Leukemia, The University of Texas M.D. Anderson Cancer Center, Houston, TX

[†]Department of Medicine II, Hematology/Oncology, Goethe University, Frankfurt, Germany

[‡]IRCCS Ospedale San Raffaele and Università Vita-Salute San Raffaele, Milan, Italy

Abstract

B-cell receptor (BCR) signaling is a central pathogenetic pathway in chronic lymphocytic leukemia (CLL). Most CLL cells express BCRs of IgM and IgD isotypes, but the contribution of these isotypes to functional responses remains incompletely defined. We therefore investigated differences between IgM and IgD signaling in freshly isolated peripheral blood CLL cells and in CLL cells cultured with nurselike cells (NLC), a model that mimics the lymph node microenvironment. IgM signaling induced prolonged activation of ERK kinases, promoted CLL cell survival, CCL3 and CCL4 chemokine secretion, and down-regulation of BCL6, the transcriptional repressor of *CCL3*. In contrast, IgD signaling induced activation of the cytoskeletal protein HS1, along with F-actin polymerization, which resulted in rapid receptor internalization, and failure to support downstream responses including CLL cell survival and chemokine secretion. IgM and IgD receptor down-modulation, HS1 and ERK activation, chemokine secretion and BCL6 down-regulation were also observed when CLL cells were co-cultured with NLC. The BTK kinase inhibitor ibrutinib effectively inhibited both, IgM and IgD isotype signaling. In conclusion, through a variety of functional readouts, we demonstrate very distinct outcomes of IgM and IgD isotype activation in CLL cells, providing novel insight into the regulation of BCR signaling in CLL.

Introduction

B cell receptor (BCR) signaling is now recognized as a central pathway in CLL pathogenesis (1) based on preclinical studies that demonstrated the importance of BCR activation for survival and proliferation of CLL cells *in vitro* (reviewed in (2)), and in mouse models of CLL (reviewed in (3)). The vast majority of CLL patients treated with Bruton's tyrosine kinase (BTK) or phosphoinositide 3-kinase delta (PI3Kδ) inhibitors (ibrutinib, idelalisib),

Address correspondence and reprint requests to Dr. Jan Burger, MD. PhD., Department of Leukemia, Unit 148, The University of Texas MD Anderson Cancer Center, PO Box 301402, Houston, TX 77230-1402; jaburger@mdanderson.org.

Disclosures. S.O.B and J.A.B received research funding from Pharmacyclics.

which primarily target BCR signaling, achieve durable responses, corroborating the relevance of BCR signaling in CLL pathogenesis (reviewed in (4)).

IgM and IgD receptor isotypes are co-expressed on mature B cells and their function in B-cell development and maturation is widely interchangeable, as demonstrated in IgM (5) and IgD (6) knock-out mouse models. The two isotypes bear the same antigenic specificity and differ only in terms of their heavy chains, IgMs carry mu (μ) and IgDs carry delta (δ) heavy chains (7). Most CLL cells express both IgMs and IgDs, (8–10) and several studies characterized the importance of IgM BCRs for CLL cell survival, cell-cycle entry, and proliferation (9, 11–13). The function of IgD in CLL has also been studied, with controversial results, mostly related to the effects of IgD stimulation on either inducing cell survival (14), or rather apoptosis (15). The mutational status of immunoglobulin heavy chain variable (*IGHV*) genes has strong prognostic significance (16, 17), and CLL cases carrying unmutated BCRs (U-CLL) show more aggressive disease features than mutated CLL (M-CLL). IgM responsiveness typically increases in U-CLL cases (8, 18, 19), while such differential responses are generally not seen after IgD stimulation (8–10).

BCR triggering activates a complex signaling cascade including upstream kinases, such as the SRC-kinase LYN, spleen tyrosine kinase (SYK), BTK and PI3Kδ, which transduce signals to cytoskeletal activators, such as hematopoietic cell-specific Lyn-substrate 1 (HS1) (20–22), and downstream effectors, including AKT and extracellular signal-regulated (ERK) kinases (23, 24). Another response to BCR stimulation is the production of C-C motif ligand (CCL)3 and CCL4 chemokines (25, 26), which are released at high concentrations by CLL cells after IgM stimulation, as well as in co-culture with nurselike cells (NLC), a CLL lymph node microenvironment model (27, 28). CCL3 and CCL4 secretion by CLL cells has been linked to the recruitment of accessory cells (T cells and monocytes/macrophages) for cognate interactions with activated and/or proliferating CLL cells within secondary lymphatic tissues (25, 29, 30), which is similar to the function of these chemokines during normal adaptive immune responses.

The aim of the present study was to analyze functional differences between IgM and IgD isotypes in the outcome of the BCR response, and to characterize the NLC-mediated activation of BCR signaling in CLL.

Materials and Methods

Primary samples and reagents

Peripheral blood (PB) samples were obtained from previously untreated patients fulfilling diagnostic and immunophenotypic criteria for CLL at the Leukemia Department at MD Anderson Cancer Center after informed consent and Institutional Review Board approval (Table I). All functional assays were performed on fresh CLL B cells, negatively selected from PB samples by EasySep Human B cell enrichment kit (StemCell Technologies, Vancouver, Canada), isolated by density gradient centrifugation over Ficoll-Plaque (GE Healthcare, Little Chalfont, UK), and cultured at 10^7 cells/mL in RPMI 1640 medium supplemented with 10% Fetal Bovine Serum (FBS; Gibco, Waltham, MA), and penicillin-streptomycin-L-Glutamine solution (Corning Inc., Corning, NY) (complete RPMI). Purity of

all preparations was ≥ 95%, as assessed by CD19 and CD5 positivity by flow cytometry. Polyclonal goat F(ab')$_2$ fragments to human IgM, to human IgD or to human kappa light chain (Southern Biotechnology, Birmingham, AL) were used for cell stimulation (anti-IgM, anti-IgD, anti-Igκ), and were dialyzed against PBS prior to use in Slide-A-Lyzer Dialysis Cassettes 10.000 MWCO (Thermo Fisher Scientific). Ibrutinib was provided by Pharmacyclics, resuspended at 100 mM in DMSO and used at a final concentration of 1 μM.

Flow cytometry

Flow cytometry staining of surface molecules (27), phospho-flow cytometry (31), viability assessment (27) and F-actin polymerization (31) were performed as previously described. Purity of B cells after isolation was tested with allophycocyanin (APC)-conjugated anti-human CD19 (clone HIB19; BD Pharmingen, San Jose, CA) and phycoerythrin (PE)-labeled anti-human CD5 (clone III 518; BD Pharmingen), or respective isotype controls (BD Pharmingen). Surface staining of IgM and IgD receptors was performed, in technical duplicates, with PE-conjugated goat polyclonal heavy chain specific anti-IgM or anti-IgD antibodies (Southern Biotechnology), or anti-IgG isotype control (Southern Biotechnology). Kappa light chain expression was evaluated with a PE-conjugated goat polyclonal anti-kappa antibody (Southern Biotechnology). For surface receptor staining before and after NLC co-culture, PBMCs were stained with CD19, and IgM and IgD MFIRs were analyzed on gated CD19$^+$ cells. For F-actin polymerization studies, 2 × 10^6 CLL cells per condition were serum starved for 2 hours, then either left untreated or exposed to 10 μg/ml anti-IgM or anti-IgD for 30 seconds, 1, 2 or 5 minutes. Next, a solution containing 40 μM fluorescein isothiocyanate (FITC)–phalloidin (Sigma-Aldrich, Saint-Louis, MO), 0.5 mg/mL 1-α-lysophosphatidylcholine (Sigma-Aldrich), and 4% paraformaldehyde (PAF; Electron Microscopy Sciences, Hatfield, PA) in PBS was added to stop the reaction and fix the cells. Cells were additionally incubated for 20 minutes at 37°C, then analyzed by flow cytometry. CLL cell viability was determined by analysis of mitochondrial transmembrane potential using 3,3′ dihexyloxacarbocyanine iodide (DiOC6; Invitrogen) and propidium iodide (PI; Sigma-Aldrich) (32) after 24, 48 or 72 hours of stimulation with 10 μg/ml anti-IgM, anti-IgD, or the combination of both. For IgM and IgD surface expression detection following BCR stimulation, 10^6 cells were treated with 10 μg/ml anti-IgM or anti-IgD F(ab')$_2$ fragments for 5 minutes, then placed on ice to stop the reaction, and washed once with FACS buffer [RPMI + 0.5% Bovine Serum Albumine (BSA)], prior to staining with PE-conjugated anti-IgM or anti-IgD heavy chain specific antibodies. To exclude any potential interference between the heavy-chain specific F(ab')$_2$ fragments used for stimulation and the antibodies used for BCR staining, we also assessed IgM and IgD surface levels after stimulation of the light chain with 10 μg/ml anti-kappa F(ab')$_2$ fragments, as previously described (10). For phospho-flow cytometry, 10^6 cells were either left untreated or exposed to 10 μg/ml anti-IgM or anti-IgD, or the combination of both, for up to 60 minutes. Cells were then fixed with 4% PAF for 10 minutes at room temperature, permeabilized with 90% methanol in PBS at −20°C overnight, washed twice in PBS supplemented with 1% BSA and stained and with Alexa 488-conjugated phospho-SRC [Tyrosine (Y)-416] clone 9A6 (1:350; EMD Millipore, Darmstadt, Germany), PE-conjugated phospho-HS1(Y397) clone D12C1 (1:100; Cell Signaling Technology, Danvers, MA), Alexa488-conjugated phospho-p44/42 [Threonine(T)202/Tyrosine (Y)204] clone D13.14.4E (1:100; Cell Signaling Technology),

or respective isotype controls (Cell Signaling Technology) for 30 minutes at 4°C. Samples were acquired with FACSCalibur (Becton Dickinson, Franklin Lakes, NJ) and data analyzed using FlowJo software Version 9.6.4 (TreeStar, Ashland, OR).

Western Blot

Western Blot was performed as previously described (21). Purified B cells were cultured at 10^7cells/mL and stimulated with 10μg/mL anti-IgM or anti-IgD for the indicated time points, then placed on ice to stop the reaction. In the NLC setting, PBMCs were cultured at 1.5×10^7cells/mL. Cells were lysed on ice for 15 minutes in RIPA Buffer (Sigma-Aldrich) containing fresh phosphatase inhibitor cocktail (phosSTOP; Roche, Mannheim, Germany) and complete protease inhibitor cocktail (Roche). Cells were then centrifuged at 13,200 rpm for 15 minutes at 4°C, and supernatants were collected and stored at −80°C until further use. Protein content was determined using the DC protein assay kit (Bio-Rad Laboratories, Hercules, CA), according to the manufacturer's instructions. 30 μg of total protein were supplemented with NuPage Sample Buffer (4x) and NuPage Sample Reducing Agent (10x) and loaded onto 4–12% sodium dodecyl sulfate-polyacrylamide gradient gels (Invitrogen), then transferred to nitrocellulose membranes (Thermo Scientific). Membranes were blocked for 15 minutes in PBS-Tween containing 5% BSA and incubated overnight with primary antibodies (diluted 1:1000) followed by species-specific horseradish peroxidase-conjugated secondary antibodies (diluted 1:5000) for 1 hour. Membranes were probed with the following primary antibodies: p44/42-MAPK (ERK1/2), phospho-p44/42 (T202/Y204), HS1 (clone D83A8), phospho-HS1 (Y397; clone D12C1), BCL6 (clone D4I2V), MYC (clone D84C12) and GAPDH (Cell Signaling Technology). Luminata Forte Western HRP Substrate (Millipore, Billerica, MA) or SuperSignal West Pico Chemiluminescent Substrate (Thermo Scientific) were used to visualize immuno-reactive bands of phospho-proteins or total proteins, respectively. Quantification of relative protein expression levels was performed by ImageJ software analysis.

ELISA

CCL3 and CCL4 chemokine levels were measured in the supernatants of purified B cells from CLL patients following stimulation with anti-IgM or anti-IgD, or the combination of both anti-IgM and anti-IgD, or in the supernatants of CLL cells after 14 days of co-culture with NLC by quantitative ELISA according to the manufacturer's instructions (Quantikine, R&D Systems, Minneapolis, MN).

CLL-NLC co-cultures

PBMCs, isolated by density gradient centrifugation over Ficoll-Plaque, were seeded at 1.5×10^7/mL in complete RPMI medium and utilized to generate NLC, as previously described (25, 27). Co-cultures were used for further experiments only when ≥ 85% CLL viability was detected by flow cytometry after 14 days of CLL-NLC co-culture. After 14 days of CLL-NLC co-culture, CLL cells were removed from NLC by repetitive washes in complete RPMI, centrifuged and resuspended at 1.5×10^7/mL, prior to culture for up to 72 hours in the absence of NLC.

Statistical analyses

Statistics were performed using GraphPad Prism software, version 6.0b for Macintosh. Two-tailed paired or unpaired Student's t tests, or Mann-Whitney tests were used for comparison, as appropriate. A P value lower than 0.05 was considered as statistically significant.

Results

Compared to IgM, IgD stimulation induces strong HS1 activation and F-actin polymerization

During the course of the study, 84 fresh CLL samples (42 M-CLL, 42 U-CLL), were analyzed for IgM and IgD expression (Fig. 1, Table I). IgM and IgD expression were both significantly higher in U-CLL as compared to M-CLL (Fig. 1, P(IgM)<0.0001; P(IgD)=0.0088). The mean relative expression of IgM was 83.38±8.71 for U-CLL and 35.28±5.19 for M-CLL; the mean relative IgD expression was 55.60±6.37 for U-CLL and 35.12±4.48 for M-CLL.

We dissected upstream and downstream signaling events in representative subgroups of U-CLL and M-CLL (Table SI), and started by analyzing the activation of the BCR-proximal cytoskeletal protein HS1 after anti-IgM and anti-IgD stimulation by flow cytometry (Fig. 2A, 2B, S1A) and Western Blot analysis (Fig. 2C, S1B) of Y397 phosphorylation. Seven U-CLL and 5 M-CLL cases were analyzed by flow cytometry, and 5 cases per subset were analyzed by Western Blot. We noted robust HS1 activation 2 and 5 minutes after anti-IgD stimulation in U-CLL (Fig. 2A, 2B, 2C), as compared to IgM (Fig. 2B; $P(2')$=0.034; $P(5')$=0.048). M-CLL cases showed higher baseline phosphorylation of HS1 and an overall lower relative increase in HS1 phosphorylation after both IgM and IgD stimulation (Fig. S1A, S1B), as compared to U-CLL.

As another readout for cytoskeletal activation following BCR stimulation, we measured F-actin polymerization after IgM and IgD stimulation in 4 U-CLL (Fig. 2D) and 4 M-CLL cases (Fig. S1C) and noted stronger F-actin polymerization following IgD stimulation, when compared to IgM stimulation, which peaked 30 seconds after stimulation, reaching significance in U-CLL cases (Fig. 2D; P=0.045).

Compared to IgM, IgD surface levels are rapidly reduced following stimulation

Since F-actin polymerization is a critical event in antigen-mediated receptor endocytosis (33), we then asked whether IgM and IgD receptors would show a distinct pattern of receptor internalization following stimulation. We tested both anti-IgM and anti-IgD effects on IgM and IgD expression, respectively, in 9 U-CLL and 6 M-CLL cases (Fig. S1D). We also analyzed IgM and IgD expression following stimulation of the light chain of 4 U-CLL Igκ^+ samples (Fig. 2E, 2F). Although IgM receptors were down-modulated in both U-CLL (Fig. S1D; P=0.017) and M-CLL cases (Fig. S1D; P=0.01), IgD down-modulation was much more pronounced (Fig. S1D; P(U-CLL)= 0.0009; P(M-CLL)=0.0007), and this effect was also evident when stimulation was performed through the Igκ light chain (Fig. 2F).

IgM stimulation induces prolonged activation of ERK kinases

We then analyzed the kinetics of ERK kinases activation after IgM and IgD stimulation in 5 U-CLL (Fig. 3) and 5 M-CLL cases (Fig. S2), by flow cytometry and Western Blot analysis. We observed prolonged phosphorylation of ERK kinases for up to 60 minutes following IgM stimulation of U-CLL (Fig. 3B, $P(15', 30', 60')=0.016$); IgD activation was more transient, with an earlier rebound of phospho-ERK levels after approximately 15 minutes following stimulation. Similar activation kinetics were observed by Western Blot analysis (Fig. 3C). Consistent to the pattern observed for HS1 activation, U-CLL cases were overall more responsive to both IgM and IgD (Fig. 3B, 3C) than M-CLL (Fig. S2A, S2B), and higher baseline phospho-ERK levels were observed in M-CLL (Fig. S2B), when compared to U-CLL (Fig. 3C).

Ibrutinib interferes with IgM and IgD signaling activation

We then tested the effects of treatment with the BTK kinase inhibitor ibrutinib on IgM and IgD- induced activation of SRC-Y416, used as a surrogate marker for LYN kinase activity, HS1-Y397 and ERK-T202/Y204, in 4 U-CLL cases (Fig. 4). We chose to test LYN as the main kinase responsible for HS1 phosphorylation (21), and a known additional target of ibrutinib (34). Western Blot analysis was used to verify inhibition of the auto-phosphorylation site on BTK (Y223) (data not shown). Ibrutinib interfered with the activation of LYN, HS1 and ERK, up to 60 minutes following anti-IgM (Fig. 4A, 4C, 4E) or anti-IgD (Fig. 4B, 4D, 4F) stimulation, and also reduced baseline activation of both HS1 (Fig 4C, 4D) and ERK (Fig. 4E, 4F).

IgM, but not IgD stimulation, induces chemokine secretion and BCL6 down-regulation

We quantified CCL3 and CCL4 chemokine secretion by CLL cells after a 24-hour stimulation with anti-IgM or anti-IgD in the supernatants of 7 U-CLL and 5 M-CLL samples. High concentrations of CCL3 (Fig. 5A) and CCL4 (Fig. 5B) were detected after IgM, but not after IgD stimulation. Low, if any, production of CCL3 (Fig. S3A) and CCL4 (Fig. S3B) was detected after stimulation of M-CLL cases. BCL6 protein is an established transcriptional repressor for the *CCL3* gene (35), which is known to be targeted for proteasomal degradation after IgM stimulation in Burkitt's lymphoma cells (36). We therefore modeled the kinetics of BCL6 degradation following anti-IgM and anti-IgD stimulation, and concomitantly measured CCL3 chemokine secretion in 3 U-CLL and 3 M-CLL cases. We observed down-regulation of BCL6 at 6 and 9 hours following IgM stimulation of U-CLL (Fig. 5C, 5D; $P(6h)=0.009$; $P(9h)=0.008$), with a concomitant increase in CCL3 production (Fig. 5E). Low, if any, down-modulation of BCL6 was observed in M-CLL (Fig. S3C, S3D), as well as minor CCL3 secretion (Fig. S3E). Similar patterns of BCL6 down-modulation were observed in 6 additional cases (3 U-CLL, 3 M-CLL) with a polyclonal anti-BCL6 antibody (data not shown).

CLL cell survival is mainly promoted by IgM stimulation

We measured CLL cell viability after 48 hours of anti-IgM or anti-IgD stimulation in 13 U-CLL and 13 M-CLL (Fig. 6). In contrast to IgD, IgM stimulation significantly increased U-CLL cell viability. The mean relative viability of U-CLL cells after anti-IgM stimulation was

185 ± 19.6%, compared to 113.9 ± 6.6% after anti-IgD stimulation (Fig. 6B, mean ± SEM, P =0.0001). M-CLL cell viability was less affected by IgM stimulation. Ibrutinib treatment (1μM) significantly reduced IgM-induced survival of 7 U-CLL cases (Figure 6A and 6C, P=0.018).

Combination of IgM and IgD stimulation increases early, but not long-term funstional responses

Since IgM and IgD receptors have the same antigenic specificity, and are therefore expected to be concomitantly engaged *in vivo*, we then tested whether combination of IgM and IgD receptor stimulation had an effect on early signaling events, including HS1 and ERK phosphorylation, or long-term functional responses, such as CCL3 chemokine secretion and CLL survival (Fig. 7). We observed increased phosphorylation of HS1 protein at 2 and 5 minutes following stimulation with combined anti-IgM and anti-IgD in 5 U-CLL cases (Fig. 7A), as compared to each stimulation alone. Similarly, ERK phosphorylation was increased up to 60 minutes following stimulation with combined anti-IgM and anti-IgD, as analyzed on 4 U-CLL cases (Fig. 7B). A modest, if any, increase in CCL3 chemokine secretion (Fig. 7C), CCL4 secretion (data not shown) and CLL viability (Fig. 7D), was observed when IgM and IgD were concomitantly stimulated, as compared to IgM stimulation alone.

BCR signaling activation in the NLC co-culture system

Co-culture with NLC supports CLL cell survival (25, 27) 28), chemokine secretion (25, 27), and a BCR signaling signature by gene expression profiling (25), suggesting that NLC engage CLL-BCRs. We therefore tested the features of BCR signaling in CLL-NLC co-culture, which represents an *in vitro* model of the lymph node microenvironment conditions. We analyzed IgM and IgD expression on 4 U-CLL cells before and after 14 days of co-culture with NLC (Fig. 8A, 8B). Then, CLL cells were removed from the NLC co-culture and BCR surface expression was analyzed for up to 72 hours after removal. We noted significant down-regulation of IgM and IgD after NLC contact in 4 U-CLL cases. IgM levels were significantly down-modulated after 14 days of CLL-NLC co-culture (Fig. 8B, P=0.038), and recovered at 48 hours following *in vitro* culture in the absence of NLC (Fig. 8B, P=0.039), reaching pre-exposure levels after 72 hours (Fig. 8B, P=0.0071). IgD levels also showed a similar pattern of down-regulation (Fig. 8B, P=0.021), and re-expression. Robust HS1 and ERK activation was detected in 4 U-CLL cases after NLC co-culture (Fig. 8C), whereas phosphorylation levels declined when CLL cells were cultured without NLC. We also detected high levels of CCL3 (Fig. 8D, P=0.0062) and CCL4 (data not shown) chemokines in supernatants of U-CLL cells co-cultured with NLC, which were lower in M-CLL cases. Interestingly, we also observed down-regulation of BCL6 protein after 14 days of CLL-NLC co-culture, which was particularly evident in U-CLL cases (Fig. 8E, 8F; P=0.011). U-CLL cells also displayed higher induction of MYC protein, in particular of the higher molecular weight isoform (Fig. 8E, 8F; P=0.047), which served as a surrogate marker for BCR activation in the CLL lymph node microenvironment (37).

Discussion

CLL cells express both IgM and IgD BCRs carrying the same antigenic specificity, but the contribution of these different isotypes to BCR signaling responses remains incompletely understood. Here, we show different outcomes of BCR signaling after IgM or IgD receptor stimulation, by dissecting proximal and downstream signaling events through a number of functional assays, which we exclusively performed on freshly isolated CLL cells. We observed rapid and robust activation of the cytoskeletal protein HS1 (Fig. 2B, 2C), together with F-actin polymerization (Fig. 2D), and subsequent receptor internalization (Fig. 2F, S1D) after IgD stimulation. HS1 activation and cytoskeletal remodeling are important early events after antigen engagement by the BCR (21, 38, 39), which favor early signalosome assembly and occur prior to antigen internalization and signal transduction (40). Our data suggest that IgDs are primarily involved in these early stages of BCR pathway activation in CLL.

In contrast to IgD, IgM signaling induced prolonged downstream activation of ERK kinases, up to 60 minutes following receptor engagement (Fig. 3), consistent with a previous study (9). The rapid internalization of IgD receptors (Fig. 2F, S1D) may, at least in part, explain the transient nature of IgD responses, considering that surface BCR retention after stimulation prolongs signal transduction, as reported for normal (41, 42) and leukemic (43) B cells. In accordance with previous reports (8, 18, 19, 21, 24), U-CLL cases expressed higher IgM surface levels and were more responsive to IgM stimulation than M-CLL, and M-CLL displayed higher baseline phospho-HS1 and phospho-ERK levels. Low IgM responsiveness and higher baseline phosphorylation of signaling proteins, in particular ERK kinases (23, 24), are features of anergic B cells, which mainly belong to the M-CLL subset of patients.

We observed higher IgD responsiveness of U-CLL cases (Fig. 2, 3) compared to M-CLL (Fig. S1, S2), which correlated with higher IgD expression on U-CLL cells (Fig. 1). The prognostic relevance of high IgD responsiveness was previously proposed (44), and it can be inferred that *in vivo*, where concomitant engagement of IgM and IgD is the expected mode of stimulation, IgDs contribute to the initiation of IgM signaling, leading to an overall stronger BCR signaling response in U-CLL, as compared to M-CLL cells. Consistently, when IgM and IgD stimulations were combined, we observed increased activation of proximal BCR signaling, including HS1 and ERK phosphorylation (Fig. 7A, 7B), as compared to each stimulation alone, whereas long-term functional responses, including chemokine secretion (Fig. 7C) and viability (Fig. 7D) were less affected by concomitant stimulation of both receptors, as compared to anti-IgM alone.

It is relevant to point out that the Fab stimulating reagents that are used in these and previously published *in vitro* studies (8–15, 18, 19, 45) differ from the ligands that CLL-BCRs encounter *in vivo*, and that additional characteristics of the stimulating antigen, including affinity (46, 47) and valency (48, 49), may influence the BCR signaling outcome.

The most differential responses after IgM or IgD stimulation of CLL cells were effects on viability and secretion of CCL3 and CCL4 chemokines (25, 26). Both, CLL viability (Fig. 6,

7D) and chemokine secretion (Fig. 5, S3, 7C) were mainly supported by IgM, but not by IgD stimulation. Interestingly, we noted that the *CCL3* transcriptional repressor BCL6 (35) was down-regulated following IgM stimulation with similar kinetics as CCL3 secretion by U-CLL cells (Fig. 5). Information about BCL6 expression in CLL is limited, and mainly related to *BCL6* gene mutations (50–53); our data suggest that BCL6 may be involved in the regulation of CCL3 production in CLL.

In NLC co-cultures, we noted significant down-regulation of surface IgM and IgD (Fig. 8A, 8B), which recovered during 72 hours of culture in the absence of NLC, consistent with the pattern of BCR recovery observed when CLL cells are cultured *in vitro* in the absence of antigenic stimulation (10). We hypothesize that NLC expose antigens that can trigger CLL-BCRs, as previously described (54), providing an explanation for the down-modulation of both IgM and IgD receptors. We also detected HS1 and ERK activation on CLL cells after 14 days of co-culture on NLC (Fig. 8C), measured high levels of CCL3 chemokine (Fig. 8D) and observed BCL6 protein down-regulation (Fig. 8E, 8F) in CLL-NLC co-cultures derived from U-CLL, thus recapitulating the functional outcomes of BCR stimulation in the absence of NLC. Although it was not possible to investigate short term BCR signaling responses in this long-term co-culture system, these data suggest that IgM and IgD may both be engaged and involved in BCR signaling activation in CLL cells when in co-culture with NLC.

In conclusion, IgM signaling induces durable and robust signaling responses that result in CLL survival, chemokine production and down-regulation of BCL6 (Fig. 9). In contrast, IgDs contribute primarily to proximal BCR signaling and to activation of the cytoskeleton, which results in rapid receptor internalization and transient downstream responses (Fig. 9). BCR down-modulation, signaling protein activation, chemokine secretion and BCL6 down-regulation are also observed when CLL cells are co-cultured with NLC (Fig. 8). Of note, the BTK kinase inhibitor ibrutinib interferes with both IgM and IgD signaling (Figure 4 and 6), consistent with known effects of ibrutinib on CLL cell viability (31), chemokine secretion (31, 55), and activation of the CLL cytoskeleton (31, 56, 57).

Collectively, our data provide insight into the differential regulation of BCR signaling in CLL, with clearly distinct response patterns following stimulation of IgM and IgD receptors.

Supplementary Material

Refer to Web version on PubMed Central for supplementary material.

Acknowledgments

The work was supported by a Leukemia & Lymphoma Society Scholar Award in Clinical Research (J.A.B.), and the MD Anderson's Moon Shot Program in CLL. This research is also supported in part by the MD Anderson Cancer Center Support Grant CA016672.

We are grateful to Stefan Koehrer and Julia Hoellenriegel for helpful discussion.

References

1. Burger JA, Chiorazzi N. B cell receptor signaling in chronic lymphocytic leukemia. Trends Immunol. 2013; 34:592–601. [PubMed: 23928062]

2. Stevenson FK, Forconi F, Packham G. The meaning and relevance of B-cell receptor structure and function in chronic lymphocytic leukemia. Semin Hematol. 2014; 51:158–167. [PubMed: 25048780]

3. Simonetti G, Bertilaccio MT, Ghia P, Klein U. Mouse models in the study of chronic lymphocytic leukemia pathogenesis and therapy. Blood. 2014; 124:1010–1019. [PubMed: 25006127]

4. Ten Hacken E, Burger JA. Microenvironment interactions and B-cell receptor signaling in Chronic Lymphocytic Leukemia: Implications for disease pathogenesis and treatment. Biochimica et biophysica acta. 2016; 1863:401–413. [PubMed: 26193078]

5. Lutz C, Ledermann B, Kosco-Vilbois MH, Ochsenbein AF, Zinkernagel RM, Kohler G, Brombacher F. IgD can largely substitute for loss of IgM function in B cells. Nature. 1998; 393:797–801. [PubMed: 9655395]

6. Roes J, Rajewsky K. Immunoglobulin D (IgD)-deficient mice reveal an auxiliary receptor function for IgD in antigen-mediated recruitment of B cells. The Journal of experimental medicine. 1993; 177:45–55. [PubMed: 8418208]

7. Surova E, Jumaa H. The role of BCR isotype in B-cell development and activation. Advances in immunology. 2014; 123:101–139. [PubMed: 24840949]

8. Lanham S, Hamblin T, Oscier D, Ibbotson R, Stevenson F, Packham G. Differential signaling via surface IgM is associated with VH gene mutational status and CD38 expression in chronic lymphocytic leukemia. Blood. 2003; 101:1087–1093. [PubMed: 12393552]

9. Krysov S, Dias S, Paterson A, Mockridge CI, Potter KN, Smith KA, Ashton-Key M, Stevenson FK, Packham G. Surface IgM stimulation induces MEK1/2-dependent MYC expression in chronic lymphocytic leukemia cells. Blood. 2012; 119:170–179. [PubMed: 22086413]

10. Mockridge CI, Potter KN, Wheatley I, Neville LA, Packham G, Stevenson FK. Reversible anergy of sIgM-mediated signaling in the two subsets of CLL defined by VH-gene mutational status. Blood. 2007; 109:4424–4431. [PubMed: 17255355]

11. Bernal A, Pastore RD, Asgary Z, Keller SA, Cesarman E, Liou HC, Schattner EJ. Survival of leukemic B cells promoted by engagement of the antigen receptor. Blood. 2001; 98:3050–3057. [PubMed: 11698290]

12. Petlickovski A, Laurenti L, Li X, Marietti S, Chiusolo P, Sica S, Leone G, Efremov DG. Sustained signaling through the B-cell receptor induces Mcl-1 and promotes survival of chronic lymphocytic leukemia B cells. Blood. 2005; 105:4820–4827. [PubMed: 15728130]

13. Paterson A, Mockridge CI, Adams JE, Krysov S, Potter KN, Duncombe AS, Cook SJ, Stevenson FK, Packham G. Mechanisms and clinical significance of BIM phosphorylation in chronic lymphocytic leukemia. Blood. 2012; 119:1726–1736. [PubMed: 22160382]

14. Zupo S, Massara R, Dono M, Rossi E, Malavasi F, Cosulich ME, Ferrarini M. Apoptosis or plasma cell differentiation of CD38-positive B-chronic lymphocytic leukemia cells induced by cross-linking of surface IgM or IgD. Blood. 2000; 95:1199–1206. [PubMed: 10666191]

15. Tavolaro S, Peragine N, Chiaretti S, Ricciardi MR, Raponi S, Messina M, Santangelo S, Marinelli M, Di Maio V, Mauro FR, Del Giudice I, Foa R, Guarini A. IgD cross-linking induces gene expression profiling changes and enhances apoptosis in chronic lymphocytic leukemia cells. Leuk Res. 2013; 37:455–462. [PubMed: 23337402]

16. Hamblin TJ, Davis Z, Gardiner A, Oscier DG, Stevenson FK. Unmutated Ig V(H) genes are associated with a more aggressive form of chronic lymphocytic leukemia. Blood. 1999; 94:1848–1854. [PubMed: 10477713]

17. Damle RN, Wasil T, Fais F, Ghiotto F, Valetto A, Allen SL, Buchbinder A, Budman D, Dittmar K, Kolitz J, Lichtman SM, Schulman P, Vinciguerra VP, Rai KR, Ferrarini M, Chiorazzi N. Ig V gene mutation status and CD38 expression as novel prognostic indicators in chronic lymphocytic leukemia. Blood. 1999; 94:1840–1847. [PubMed: 10477712]

18. Allsup DJ, Kamiguti AS, Lin K, Sherrington PD, Matrai Z, Slupsky JR, Cawley JC, Zuzel M. B-cell receptor translocation to lipid rafts and associated signaling differ between prognostically important subgroups of chronic lymphocytic leukemia. Cancer Res. 2005; 65:7328–7337. [PubMed: 16103084]

19. Guarini A, Chiaretti S, Tavolaro S, Maggio R, Peragine N, Citarella F, Ricciardi MR, Santangelo S, Marinelli M, De Propris MS, Messina M, Mauro FR, Del Giudice I, Foa R. BCR ligation induced

by IgM stimulation results in gene expression and functional changes only in IgV H unmutated chronic lymphocytic leukemia (CLL) cells. Blood. 2008; 112:782–792. [PubMed: 18487510]

20. Scielzo C, Ghia P, Conti A, Bachi A, Guida G, Geuna M, Alessio M, Caligaris-Cappio F. HS1 protein is differentially expressed in chronic lymphocytic leukemia patient subsets with good or poor prognoses. J Clin Invest. 2005; 115:1644–1650. [PubMed: 15931393]
21. ten Hacken E, Scielzo C, Bertilaccio MT, Scarfo L, Apollonio B, Barbaglio F, Stamatopoulos K, Ponzoni M, Ghia P, Caligaris-Cappio F. Targeting the LYN/HS1 signaling axis in chronic lymphocytic leukemia. Blood. 2013; 121:2264–2273. [PubMed: 23325840]
22. Scielzo C, Bertilaccio MT, Simonetti G, Dagklis A, ten Hacken E, Fazi C, Muzio M, Caiolfa V, Kitamura D, Restuccia U, Bachi A, Rocchi M, Ponzoni M, Ghia P, Caligaris-Cappio F. HS1 has a central role in the trafficking and homing of leukemic B cells. Blood. 2010; 116:3537–3546. [PubMed: 20530793]
23. Muzio M, Apollonio B, Scielzo C, Frenquelli M, Vandoni I, Boussiotis V, Caligaris-Cappio F, Ghia P. Constitutive activation of distinct BCR-signaling pathways in a subset of CLL patients: a molecular signature of anergy. Blood. 2008; 112:188–195. [PubMed: 18292287]
24. Apollonio B, Scielzo C, Bertilaccio MT, Ten Hacken E, Scarfo L, Ranghetti P, Stevenson F, Packham G, Ghia P, Muzio M, Caligaris-Cappio F. Targeting B-cell anergy in chronic lymphocytic leukemia. Blood. 2013; 121:3879–3888. S3871–3878. [PubMed: 23460614]
25. Burger JA, Quiroga MP, Hartmann E, Burkle A, Wierda WG, Keating MJ, Rosenwald A. High-level expression of the T-cell chemokines CCL3 and CCL4 by chronic lymphocytic leukemia B cells in nurselike cell cocultures and after BCR stimulation. Blood. 2009; 113:3050–3058. [PubMed: 19074730]
26. Sivina M, Hartmann E, Kipps TJ, Rassenti L, Krupnik D, Lerner S, LaPushin R, Xiao L, Huang X, Werner L, Neuberg D, Kantarjian H, O'Brien S, Wierda WG, Keating MJ, Rosenwald A, Burger JA. CCL3 (MIP-1alpha) plasma levels and the risk for disease progression in chronic lymphocytic leukemia. Blood. 2011; 117:1662–1669. [PubMed: 21115978]
27. Burger JA, Tsukada N, Burger M, Zvaifler NJ, Dell'Aquila M, Kipps TJ. Blood-derived nurse-like cells protect chronic lymphocytic leukemia B cells from spontaneous apoptosis through stromal cell-derived factor-1. Blood. 2000; 96:2655–2663. [PubMed: 11023495]
28. Tsukada N, Burger JA, Zvaifler NJ, Kipps TJ. Distinctive features of "nurselike" cells that differentiate in the context of chronic lymphocytic leukemia. Blood. 2002; 99:1030–1037. [PubMed: 11807009]
29. Zucchetto A, Benedetti D, Tripodo C, Bomben R, Dal Bo M, Marconi D, Bossi F, Lorenzon D, Degan M, Rossi FM, Rossi D, Bulian P, Franco V, Del Poeta G, Deaglio S, Gaidano G, Tedesco F, Malavasi F, Gattei V. CD38/CD31, the CCL3 and CCL4 chemokines, and CD49d/vascular cell adhesion molecule-1 are interchained by sequential events sustaining chronic lymphocytic leukemia cell survival. Cancer Res. 2009; 69:4001–4009. [PubMed: 19383907]
30. Hartmann EM, Rudelius M, Burger JA, Rosenwald A. CCL3 chemokine expression by chronic lymphocytic leukemia cells orchestrates the composition of the microenvironment in lymph node infiltrates. Leukemia & lymphoma. 2015:1–9.
31. Ponader S, Chen SS, Buggy JJ, Balakrishnan K, Gandhi V, Wierda WG, Keating MJ, O'Brien S, Chiorazzi N, Burger JA. The Bruton tyrosine kinase inhibitor PCI-32765 thwarts chronic lymphocytic leukemia cell survival and tissue homing in vitro and in vivo. Blood. 2012; 119:1182–1189. [PubMed: 22180443]
32. Ozgen U, Savasan S, Buck S, Ravindranath Y. Comparison of DiOC(6)(3) uptake and annexin V labeling for quantification of apoptosis in leukemia cells and non-malignant T lymphocytes from children. Cytometry. 2000; 42:74–78. [PubMed: 10679746]
33. Song W, Liu C, Upadhyaya A. The pivotal position of the actin cytoskeleton in the initiation and regulation of B cell receptor activation. Biochimica et biophysica acta. 2014; 1838:569–578. [PubMed: 23886914]
34. Honigberg LA, Smith AM, Sirisawad M, Verner E, Loury D, Chang B, Li S, Pan Z, Thamm DH, Miller RA, Buggy JJ. The Bruton tyrosine kinase inhibitor PCI-32765 blocks B-cell activation and is efficacious in models of autoimmune disease and B-cell malignancy. Proceedings of the National Academy of Sciences of the United States of America. 2010; 107:13075–13080. [PubMed: 20615965]

35. Shaffer AL, Yu X, He Y, Boldrick J, Chan EP, Staudt LM. BCL-6 represses genes that function in lymphocyte differentiation, inflammation, and cell cycle control. Immunity. 2000; 13:199–212. [PubMed: 10981963]

36. Niu H, Ye B, Dalla-Favera R. Antigen receptor signaling induces MAP kinase-mediated phosphorylation and degradation of the BCL-6 transcription factor. Genes Dev. 1998; 12:1953–1961. [PubMed: 9649500]

37. Herishanu Y, Perez-Galan P, Liu D, Biancotto A, Pittaluga S, Vire B, Gibellini F, Njuguna N, Lee E, Stennett L, Raghavachari N, Liu P, McCoy JP, Raffeld M, Stetler-Stevenson M, Yuan C, Sherry R, Arthur DC, Maric I, White T, Marti GE, Munson P, Wilson WH, Wiestner A. The lymph node microenvironment promotes B-cell receptor signaling, NF-kappaB activation, and tumor proliferation in chronic lymphocytic leukemia. Blood. 2011; 117:563–574. [PubMed: 20940416]

38. Fleire SJ, Goldman JP, Carrasco YR, Weber M, Bray D, Batista FD. B cell ligand discrimination through a spreading and contraction response. Science. 2006; 312:738–741. [PubMed: 16675699]

39. Natkanski E, Lee WY, Mistry B, Casal A, Molloy JE, Tolar P. B cells use mechanical energy to discriminate antigen affinities. Science. 2013; 340:1587–1590. [PubMed: 23686338]

40. Hoogeboom R, Tolar P. Molecular Mechanisms of B Cell Antigen Gathering and Endocytosis. Curr Top Microbiol Immunol. 2016; 393:45–63. [PubMed: 26336965]

41. Hou P, Araujo E, Zhao T, Zhang M, Massenburg D, Veselits M, Doyle C, Dinner AR, Clark MR. B cell antigen receptor signaling and internalization are mutually exclusive events. PLoS Biol. 2006; 4:e200. [PubMed: 16719564]

42. Gazumyan A, Reichlin A, Nussenzweig MC. Ig beta tyrosine residues contribute to the control of B cell receptor signaling by regulating receptor internalization. The Journal of experimental medicine. 2006; 203:1785–1794. [PubMed: 16818674]

43. Calpe E, Codony C, Baptista MJ, Abrisqueta P, Carpio C, Purroy N, Bosch F, Crespo M. ZAP-70 enhances migration of malignant B lymphocytes toward CCL21 by inducing CCR7 expression via IgM-ERK1/2 activation. Blood. 2011; 118:4401–4410. [PubMed: 21865343]

44. Morabito F, Cutrona G, Gentile M, Fabbi M, Matis S, Colombo M, Reverberi D, Megna M, Spriano M, Callea V, Vigna E, Rossi E, Lucia E, Festini G, Zupo S, Molica S, Neri A, Ferrarini M. Prognostic relevance of in vitro response to cell stimulation via surface IgD in binet stage a CLL. Br J Haematol. 2010; 149:160–163. [PubMed: 19995391]

45. Zupo S, Isnardi L, Megna M, Massara R, Malavasi F, Dono M, Cosulich E, Ferrarini M. CD38 expression distinguishes two groups of B-cell chronic lymphocytic leukemias with different responses to anti-IgM antibodies and propensity to apoptosis. Blood. 1996; 88:1365–1374. [PubMed: 8695855]

46. Iacovelli S, Hug E, Bennardo S, Duehren-von Minden M, Gobessi S, Rinaldi A, Suljagic M, Bilbao D, Bolasco G, Eckl-Dorna J, Niederberger V, Autore F, Sica S, Laurenti L, Wang H, Cornall RJ, Clarke SH, Croce CM, Bertoni F, Jumaa H, Efremov DG. Two types of BCR interactions are positively selected during leukemia development in the Emu-TCL1 transgenic mouse model of CLL. Blood. 2015; 125:1578–1588. [PubMed: 25564405]

47. Chen SS, Batliwalla F, Holodick NE, Yan XJ, Yancopoulos S, Croce CM, Rothstein TL, Chiorazzi N. Autoantigen can promote progression to a more aggressive TCL1 leukemia by selecting variants with enhanced B-cell receptor signaling. Proceedings of the National Academy of Sciences of the United States of America. 2013; 110:E1500–1507. [PubMed: 23550156]

48. Kim KM, Reth M. The B cell antigen receptor of class IgD induces a stronger and more prolonged protein tyrosine phosphorylation than that of class IgM. The Journal of experimental medicine. 1995; 181:1005–1014. [PubMed: 7869025]

49. Ubelhart R, Hug E, Bach MP, Wossning T, Duhren-von Minden M, Horn AH, Tsiantoulas D, Kometani K, Kurosaki T, Binder CJ, Sticht H, Nitschke L, Reth M, Jumaa H. Responsiveness of B cells is regulated by the hinge region of IgD. Nature immunology. 2015; 16:534–543. [PubMed: 25848865]

50. Sahota SS, Davis Z, Hamblin TJ, Stevenson FK. Somatic mutation of bcl-6 genes can occur in the absence of V(H) mutations in chronic lymphocytic leukemia. Blood. 2000; 95:3534–3540. [PubMed: 10828040]

51. Pasqualucci L, Neri A, Baldini L, Dalla-Favera R, Migliazza A. BCL-6 mutations are associated with immunoglobulin variable heavy chain mutations in B-cell chronic lymphocytic leukemia. Cancer Res. 2000; 60:5644–5648. [PubMed: 11059755]

52. Capello D, Vitolo U, Pasqualucci L, Quattrone S, Migliaretti G, Fassone L, Ariatti C, Vivenza D, Gloghini A, Pastore C, Lanza C, Nomdedeu J, Botto B, Freilone R, Buonaiuto D, Zagonel V, Gallo E, Palestro G, Saglio G, Dalla-Favera R, Carbone A, Gaidano G. Distribution and pattern of BCL-6 mutations throughout the spectrum of B-cell neoplasia. Blood. 2000; 95:651–659. [PubMed: 10627476]

53. Maddocks KJ, Ruppert AS, Lozanski G, Heerema NA, Zhao W, Abruzzo L, Lozanski A, Davis M, Gordon A, Smith LL, Mantel R, Jones JA, Flynn JM, Jaglowski SM, Andritsos LA, Awan F, Blum KA, Grever MR, Johnson AJ, Byrd JC, Woyach JA. Etiology of Ibrutinib Therapy Discontinuation and Outcomes in Patients With Chronic Lymphocytic Leukemia. JAMA Oncol. 2015; 1:80–87. [PubMed: 26182309]

54. Binder M, Lechenne B, Ummanni R, Scharf C, Balabanov S, Trusch M, Schluter H, Braren I, Spillner E, Trepel M. Stereotypical chronic lymphocytic leukemia B-cell receptors recognize survival promoting antigens on stromal cells. PloS one. 2010; 5:e15992. [PubMed: 21209908]

55. Burger JA, Keating MJ, Wierda WG, Hartmann E, Hoellenriegel J, Rosin NY, de Weerdt I, Jeyakumar G, Ferrajoli A, Cardenas-Turanzas M, Lerner S, Jorgensen JL, Nogueras-Gonzalez GM, Zacharian G, Huang X, Kantarjian H, Garg N, Rosenwald A, O'Brien S. Safety and activity of ibrutinib plus rituximab for patients with high-risk chronic lymphocytic leukaemia: a single-arm, phase 2 study. Lancet Oncol. 2014; 15:1090–1099. [PubMed: 25150798]

56. Herman SE, Mustafa RZ, Jones J, Wong DH, Farooqui M, Wiestner A. Treatment with Ibrutinib Inhibits BTK- and VLA-4-Dependent Adhesion of Chronic Lymphocytic Leukemia Cells In Vivo. Clinical cancer research: an official journal of the American Association for Cancer Research. 2015; 21:4642–4651. [PubMed: 26089373]

57. de Rooij MF, Kuil A, Kater AP, Kersten MJ, Pals ST, Spaargaren M. Ibrutinib and idelalisib synergistically target BCR-controlled adhesion in MCL and CLL: a rationale for combination therapy. Blood. 2015; 125:2306–2309. [PubMed: 25838279]

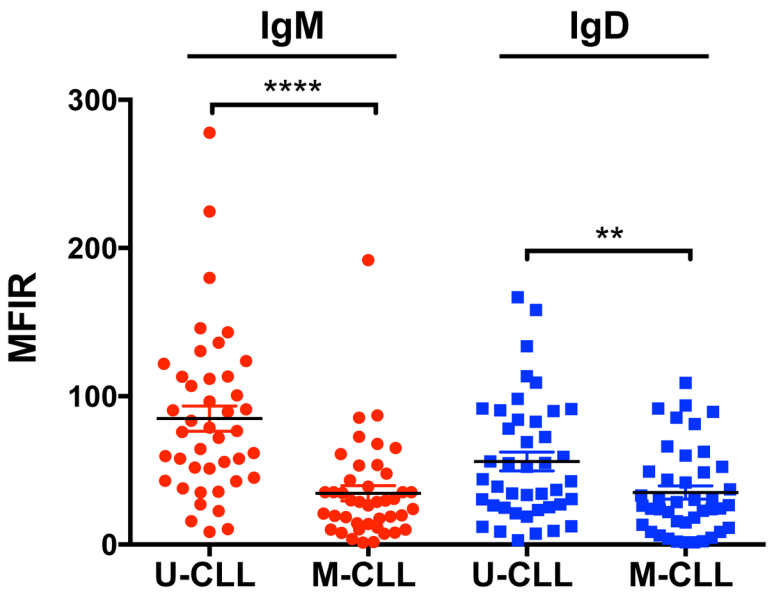

Figure 1. IgM and IgD surface expression in U-CLL and M-CLL cases

Mean ± SEM of IgM and IgD receptor expression, expressed as Mean Fluorescent Intensity Ratio (MFIR) in U-CLL (n=42), and M-CLL (n=42), ** P <0.01; **** P <0.0001; Mann-Whitney test.

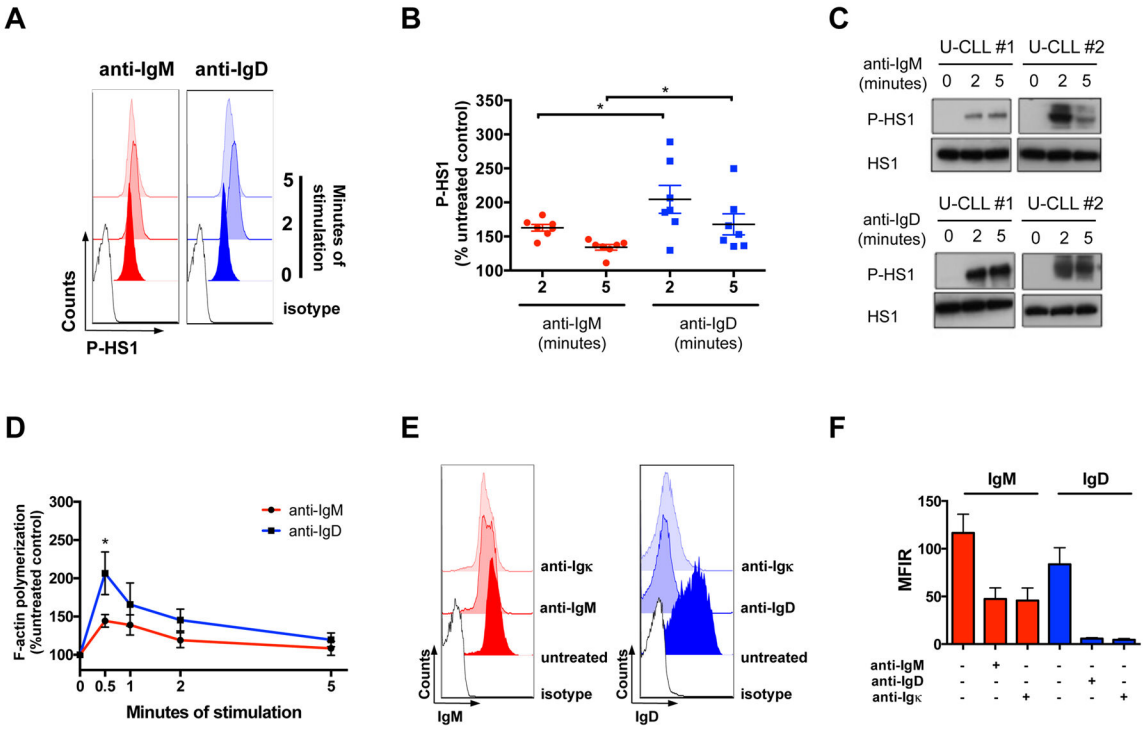

Figure 2. HS1 activation, F-actin polymerization and receptor internalization assays

(A) Representative histograms of HS1-Y397 phosphorylation (P-HS1) flow cytometry analysis at 2 and 5 minutes following anti-IgM or anti-IgD receptor stimulation in one U-CLL case. Isotypes are shown, as control. **(B)** Mean ± SEM of P-HS1, after 2 and 5 minutes of anti-IgM or anti-IgD stimulation, as analyzed by flow cytometry on 7 U-CLL cases, and expressed as percentage (%) of the untreated control. **P* <0.05; Mann-Whitney test. **(C)** Western Blot analysis of P-HS1 at the activatory tyrosine residue Y397 and HS1 total levels after 2 and 5 minutes of anti-IgM or anti-IgD stimulation. Two representative U-CLL cases (U-CLL#1, U-CLL#2) out of 5 tested are shown. **(D)** Mean ± SEM of F-actin polymerization after a period of 5 minutes of anti-IgM or anti-IgD stimulation, as analyzed on 4 U-CLL cases, and expressed as % of the untreated control. **P* <0.05; unpaired t test. **(E)** Representative histograms of IgM and IgD surface staining of one U-CLL case before and after 5 minutes of anti-IgM, anti-IgD or anti-Igκ stimulation. Isotypes are shown, as control. **(F)** Comparison of the effect of heavy chain stimulation (anti-IgM, anti-IgD) and light chain stimulation (anti-Igκ) on surface IgM and IgD levels. Mean ± SEM of IgM and IgD receptor expression, expressed as Mean Fluorescent Intensity Ratio (MFIR) before and after 5 minutes of anti-IgM, anti-IgD or anti-Igκ, as analyzed in 4 Igκ$^+$ U-CLL cases.

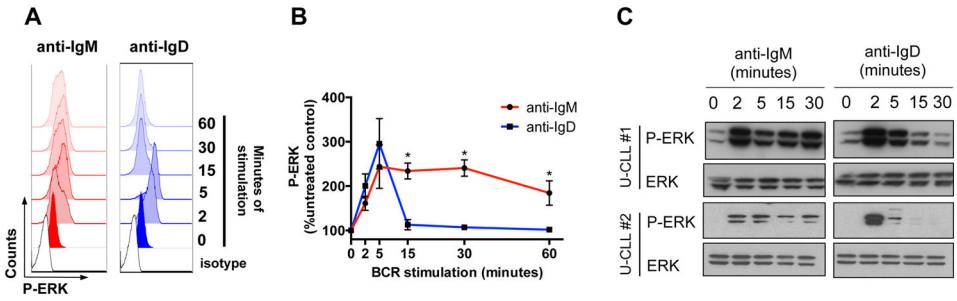

Figure 3. ERK kinases activation assays

(A) Representative histograms of ERK kinase phosphorylation (P-ERK) flow cytometry analysis at serial time points following anti-IgM or anti-IgD receptor stimulation in one U-CLL sample. Isotypes are shown, as control. **(B)** Mean ± SEM of P-ERK, at serial time points following anti-IgM or anti-IgD stimulation, as analyzed by flow cytometry on 5 U-CLL samples, and expressed as percentage (%) of the untreated control. **P* <0.05; Mann-Whitney test. **(C)** Western Blot analysis of P-ERK and ERK total levels at serial time points following anti-IgM or anti-IgD stimulation. Two representative U-CLL cases (U-CLL#1, U-CLL#2) out of 5 tested are shown.

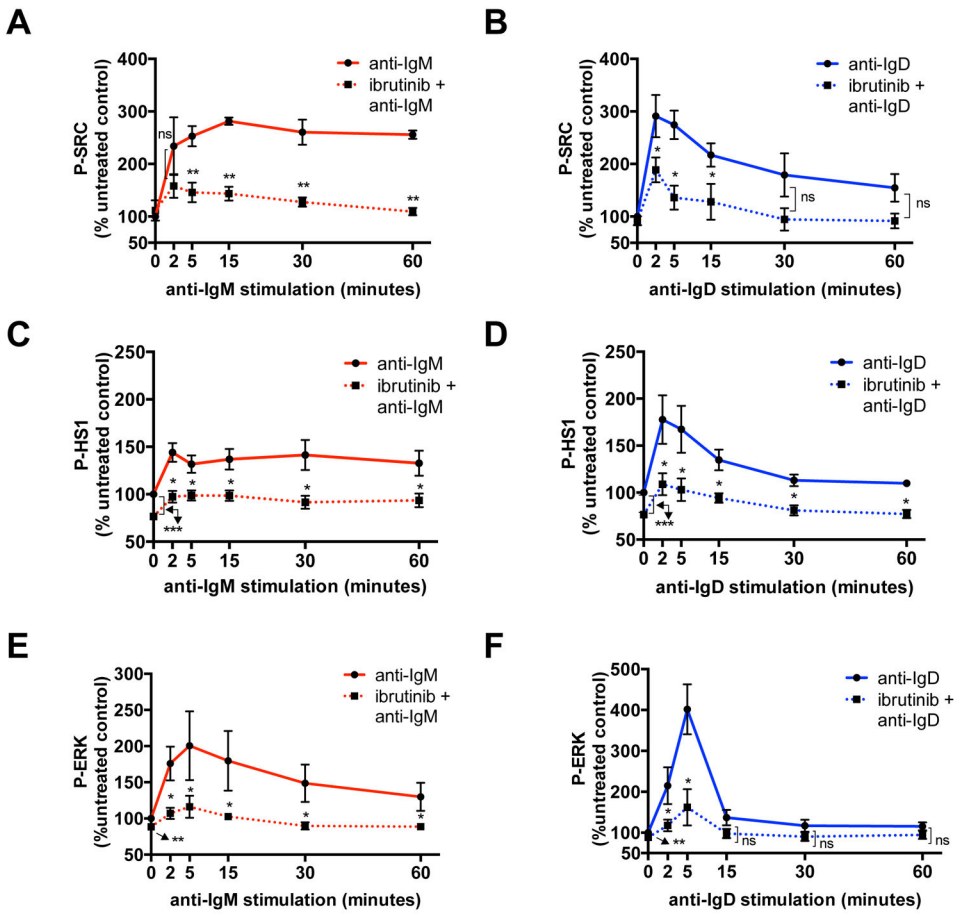

Figure 4. Phospho-flow analysis of SRC, HS1 and ERK activation after ibrutinib treatment

Mean ± SEM of **(A)** SRC-Y416, **(C)** HS1-Y397 and **(E)** ERK T202/Y204 phosphorylation at serial time points following anti-IgM stimulation, as analyzed by flow cytometry on 4 U-CLL cases in the absence or presence of 1-hour pretreatment with 1μM ibrutinib, and expressed as percentage (%) of the untreated control. Mean ± SEM of **(B)** SRC-Y416, **(D)** HS1-Y397 and **(F)** ERK T202/Y204 phosphorylation at serial time points following anti-IgD stimulation, as analyzed by flow cytometry on 4 U-CLL cases in the absence or presence of 1-hour pretreatment with 1μM ibrutinib, and expressed as percentage (%) of the untreated control. **P*<0.05; ***P*<0.01; ****P*<0.001; ns: not significant; paired t test.

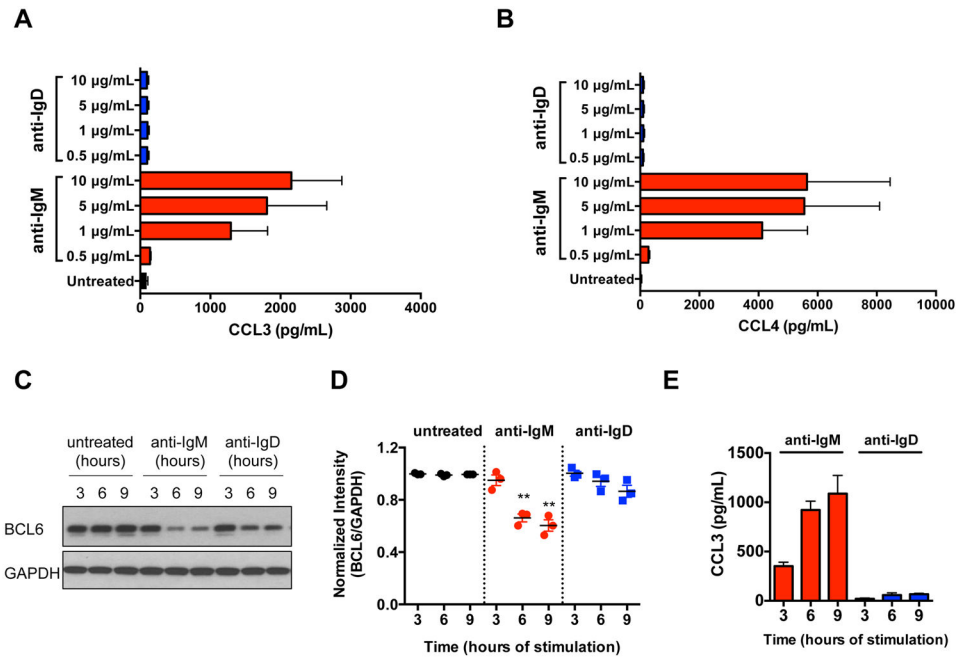

Figure 5. CCL3 and CCL4 chemokine secretion and BCL6 protein expression analyses

(A) CCL3 and **(B)** CCL4 measurement by ELISA in the supernatants of 7 U-CLL samples after a 24-hour stimulation with increasing concentrations of anti-IgM and anti-IgD. Displayed are the means ± SEM of chemokine concentrations in pg/mL. **(C)** Western Blot analysis of BCL6 protein expression at serial time points following anti-IgM or anti-IgD of a U-CLL case. GAPDH protein levels were analyzed, as loading control. A representative U-CLL case out of 3 is shown. **(D)** Quantification of BCL6 protein expression after anti-IgM or anti-IgD in 3 U-CLL cases, expressed as normalized intensity between BCL6 and GAPDH levels. $^{**}P<0.01$; paired t test with time-matched control. **(E)** CCL3 chemokine measurement in the supernatants of 3 U-CLL cases at serial time points following anti-IgM or anti-IgD stimulation. Displayed are the means ± SEM of chemokine concentrations in pg/mL.

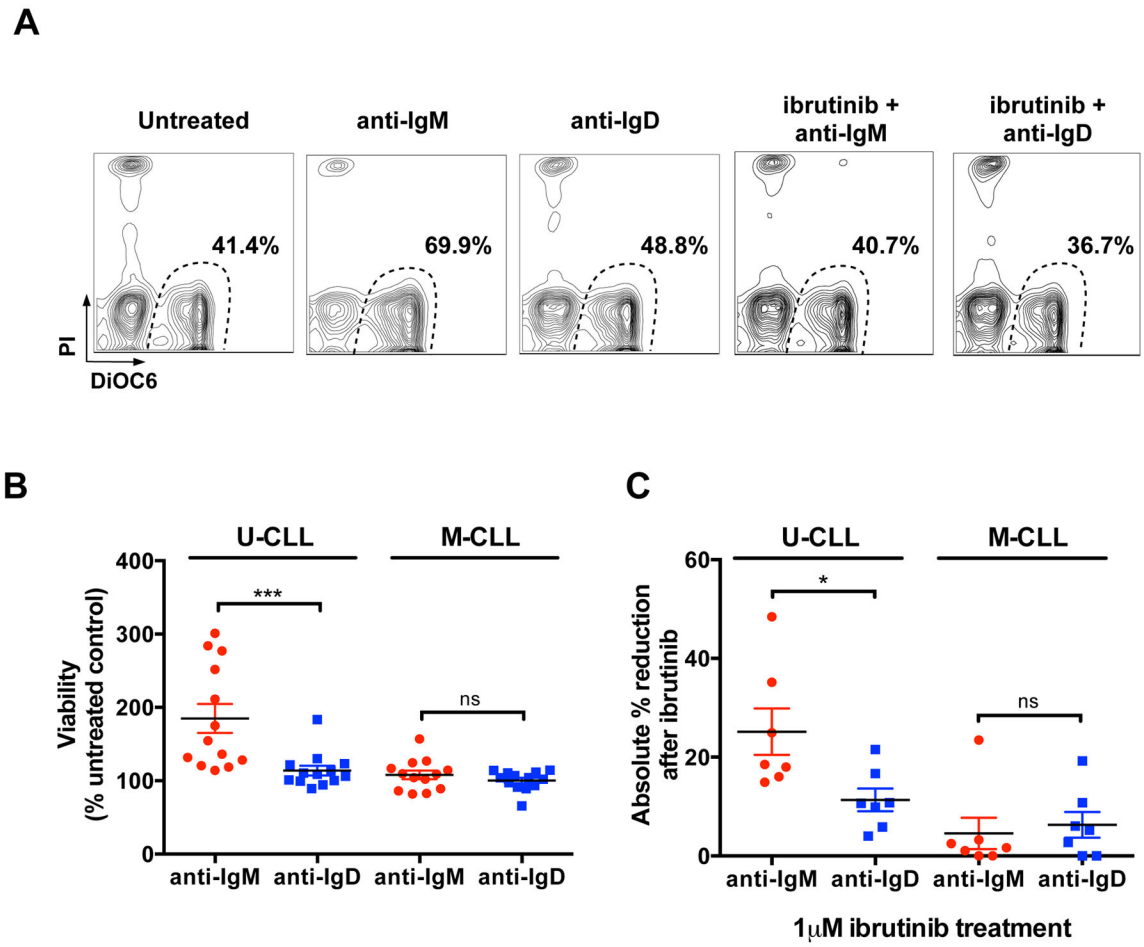

Figure 6. Viability assessment after BCR stimulation and ibrutinib treatment

(A) Representative flow cytometry contour plots of viability assessment by DiOC6 and PI staining of one U-CLL case treated with anti-IgM or anti-IgD for 48 hours in the presence or absence of 1μM ibrutinib. **(B)** Mean ± SEM of viability after 48 hours of stimulation with anti-IgM or anti-IgD, as analyzed on 13 U-CLL and 13 M-CLL cases, and expressed as percentage (%) of the untreated control. ***P <0.001; ns: not significant; Mann-Whitney test. **(C)** Mean ± SEM of the absolute % reduction in viability after ibrutinib treatment, and 48 hours stimulation with anti-IgM or anti-IgD, as analyzed on 7 U-CLL and 7 M-CLL cases. *P <0.05; ns: not significant; Mann-Whitney test.

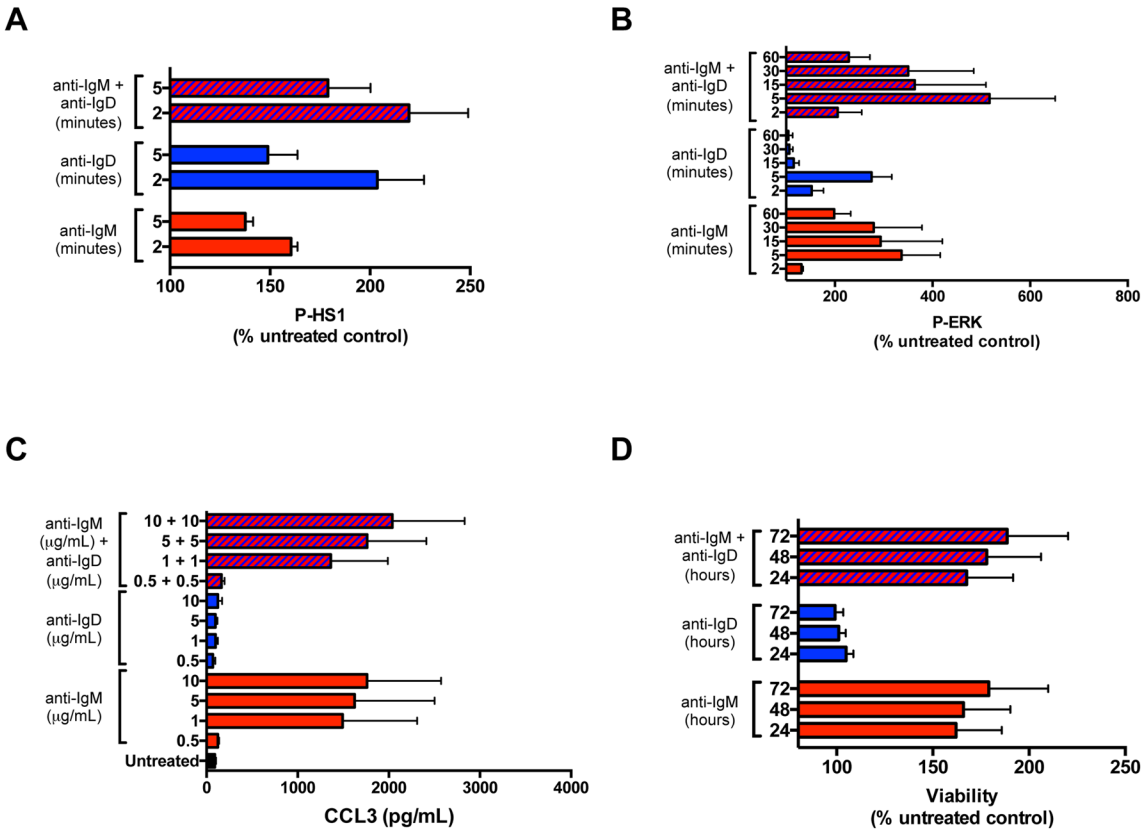

Figure 7. Functional outcomes of combination of anti-IgM and anti-IgD stimulation

(A) Mean ± SEM of HS1 phosphorylation (P-HS1), after 2 and 5 minutes of anti-IgM or anti-IgD stimulation, or the combination of both, as analyzed by flow cytometry on 5 U-CLL cases, and expressed as percentage (%) of the untreated control. **(B)** Mean ± SEM of ERK phosphorylation (P-ERK), at serial time points following anti-IgM or anti-IgD stimulation, or the combination of both, as analyzed by flow cytometry on 4 U-CLL samples, and expressed as percentage (%) of the untreated control. **(C)** CCL3 measurement by ELISA in the supernatants of 4 U-CLL samples after a 24-hour stimulation with increasing concentrations (μg/mL) of anti-IgM or anti-IgD, or the combination of both. Displayed are the means ± SEM of chemokine concentrations in pg/mL. **(D)** Mean ± SEM of viability after 24, 48, or 72 hours of stimulation with anti-IgM or anti-IgD, or the combination of both, as analyzed on 5 U-CLL cases, and expressed as percentage (%) of the untreated control.

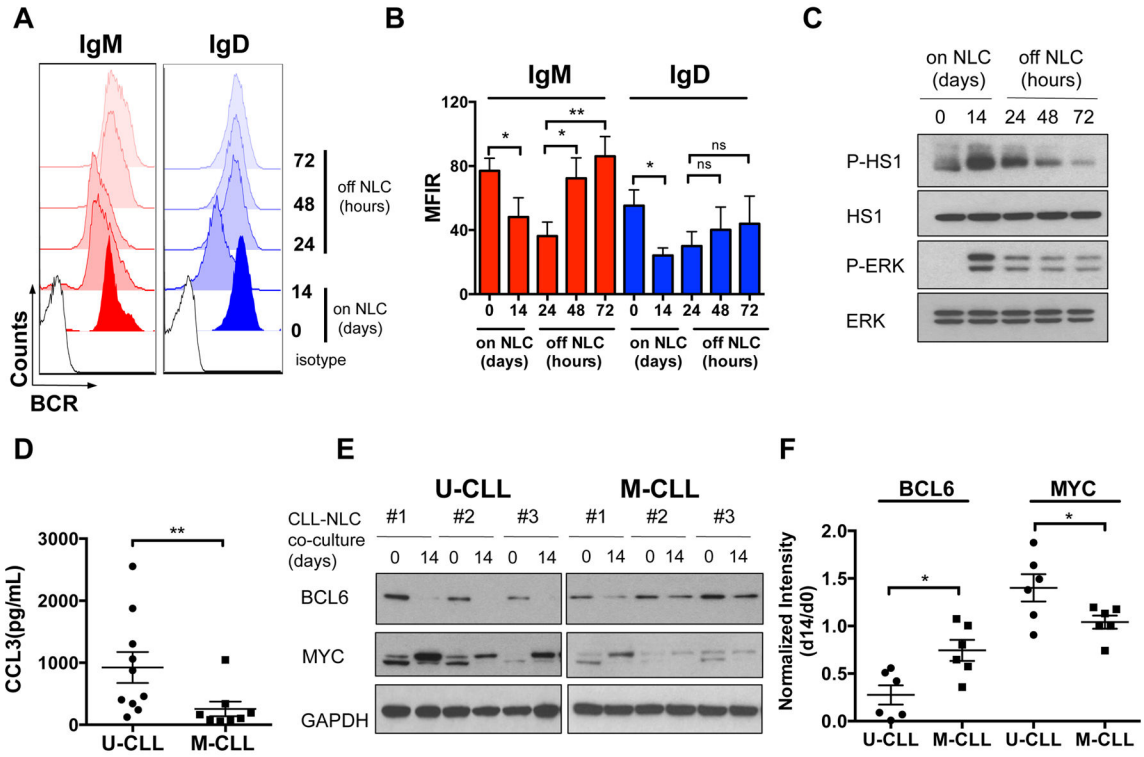

Figure 8. BCR signaling activation in the NLC co-culture system

(A) Representative histograms of flow cytometry analysis of surface IgM and IgD expression before and after 14 days of co-culture with NLCs (on NLC) and up to 72 hours of culture after removal from the CLL-NLC co-culture (off NLC), in one representative U-CLL case. Isotypes are shown, as control. **(B)** Mean ± SEM of IgM and IgD MFIR before and after 14 days of co-culture with NLC (on NLC) in 4 U-CLL and up to 72 hours of culture after removal from the CLL-NLC co-culture (off NLC). **P*<0.05; ***P*<0.01; paired t test. **(C)** Western Blot analysis of HS1 and ERK phosphorylation (P-HS1, P-ERK) and total levels before and after 14 days of co-culture with NLC (on NLC) and up to 72 hours of culture after removal from the CLL-NLC co-culture (off NLC). One representative U-CLL case out of 4 tested is shown**. (D)** Means ± SEM of CCL3 chemokine levels in pg/mL in the supernatants of CLL-NLC co-cultures of 10 U-CLL and 8 M-CLL cases after 14 days of co-culture with NLC. ***P*<0.01, Mann-Whitney test. **(E)** Western Blot analysis of BCL6 and MYC protein expression in PBMCs from U-CLL and M-CLL patients before and after 14 days of co-culture with NLC. Three representative cases per group are shown. GAPDH protein levels were analyzed, as loading control. **(F)** Relative expression of BCL6 and MYC protein after 14 days (d14) of CLL-NLC co-culture as a ratio of the levels prior to co-culture (d0) in 6 U-CLL and 6 M-CLL cases. **P* <0.05, unpaired t test.

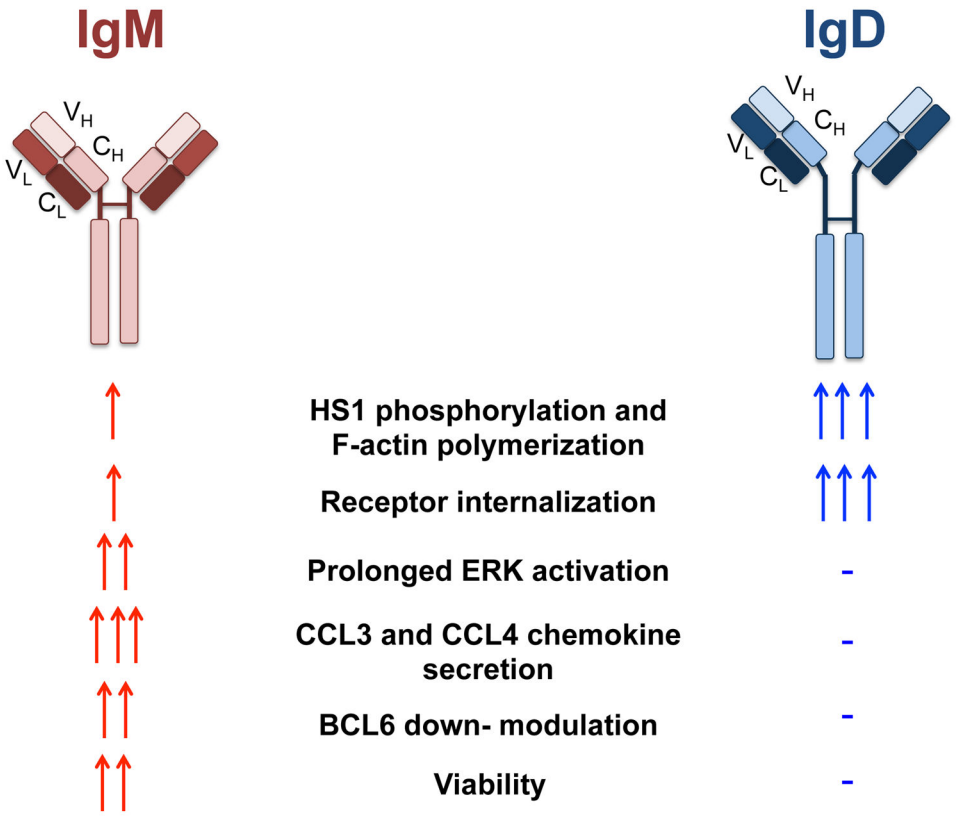

Figure 9. Schematic representation of IgM and IgD isotype functions

IgM and IgD isotype stimulation triggers very distinct signaling outcomes. IgM induces prolonged signaling activation, and is mainly responsible for CLL survival and chemokine secretion. IgD receptors, which are structurally very similar to IgM, induce strong activation of proximal signaling proteins and of the cytoskeleton, but are rapidly internalized following stimulation and fail to activate downstream responses. V_H: variable region of the heavy chain; C_H: constant region of the heavy chain; V_L: variable region of the light chain; C_L: constant region of the light chain.

Table I

Clinical and biological features of the analyzed CLL patients.

CLL	RAI stage	Age	Sex	*IGHV* status	CD38	ZAP70	Cytogenetics	IgM MFIR	IgD MFIR
1	IV	54	F	M	neg	neg	del 13q	3.70	1.51
2	I	60	M	U	neg	neg	del 11q, del13q	15.73	12.25
3	III	48	M	M	neg	pos	del 13q	60.92	85.48
4	IV	50	M	M	neg	pos	neg	11.36	24.22
5	I	74	M	U	pos	pos	del 13q	71.99	90.55
6	I	83	F	U	neg	pos	del13q, del17p	37.83	9.18
7	0	67	F	M	neg	nd	del 13q	26.35	30.10
8	I	53	M	M	neg	neg	del 13q	30.74	15.70
9	0	68	M	M	neg	nd	del 13q	19.30	26.20
10	III	56	M	U	neg	pos	neg	59.53	36.77
11	I	54	M	M	neg	nd	del 13q	87.03	49.12
12	0	49	M	M	neg	nd	del 13q	8.02	11.22
13	III	70	M	M	pos	neg	neg	43.28	14.89
14	0	55	M	U	neg	pos	nd	100.51	109.15
15	0	72	F	M	neg	nd	nd	34.76	13.33
16	0	62	M	M	neg	neg	del 13q	19.65	22.73
17	0	45	F	U	neg	pos	tri 12	91.12	38.99
18	I	71	M	M	neg	nd	del 13q	85.44	62.49
19	I	64	F	M	neg	neg	neg	18.80	37.80
20	II	68	M	U	pos	pos	neg	224.66	89.91
21	I	40	M	M	nd	nd	del 13q	67.78	91.71
22	0	54	F	M	neg	neg	del 13q	35.22	31.17
23	IV	63	M	M	neg	neg	del 13q	28.66	6.14
24	I	80	F	U	neg	pos	del 13q	83.39	44.07
25	I	60	M	U	pos	pos	del 13q, del17p	145.92	21.05
26	I	73	M	U	nd	pos	del13q	113.18	23.18
27	I	55	F	U	neg	pos	neg	43.01	30.56

CLL	RAI stage	Age	Sex	*IGHV* status	CD38	ZAP70	Cytogenetics	IgM MFIR	IgD MFIR
28	I	52	F	U	pos	pos	neg	45.00	91.67
29	I	70	F	M	nd	nd	del 13q	10.19	3.86
30	II	73	M	U	nd	nd	nd	75.83	30.45
31	0	69	F	M	neg	neg	tri12, del 13q	53.32	21.87
32	II	70	F	U	neg	pos	tri 12, del 13q, del 17p	111.78	166.79
33	III	73	F	M	pos	nd	neg	35.24	108.99
34	I	72	F	M	pos	neg	neg	10.06	23.73
35	0	66	M	M	pos	neg	tri12	1.60	1.90
36	0	69	F	M	nd	nd	nd	17.33	52.36
37	0	55	M	U	pos	nd	tri12	123.70	91.34
38	III	58	M	U	nd	nd	nd	277.85	52.43
39	II	67	M	U	pos	pos	del 11q, del13q	96.46	72.54
40	IV	66	F	U	pos	nd	del13q	130.37	133.63
41	I	59	M	M	nd	neg	del13q	20.82	51.30
42	0	70	F	M	nd	nd	neg	23.96	66.12
43	0	61	F	M	neg	neg	del13q	29.65	26.44
44	I	71	F	M	pos	neg	neg	10.06	23.73
45	I	66	F	M	neg	nd	neg	39.54	23.18
46	IV	54	M	M	neg	neg	del11q, del13q	191.78	24.07
47	I	80	F	M	nd	nd	del13q	18.43	8.45
48	II	79	M	M	neg	pos	del13q	39.01	31.87
49	I	55	F	M	neg	neg	neg	47.75	89.53
50	I	58	F	M	neg	pos	del13q	35.18	18.06
51	IV	62	M	M	neg	neg	del13q	7.36	2.15
52	I	71	M	M	neg	nd	del13q	48.57	29.67
53	I	68	M	M	pos	nd	tri12, del13q	1.20	1.39
54	0	56	F	U	pos	pos	del13q	90.45	113.44
55	II	61	F	U	neg	nd	del11q, del13q	89.40	158.21
56	I	59	F	U	neg	pos	tri12	26.96	24.72

CLL	RAI stage	Age	Sex	*IGHV* status	CD38	ZAP70	Cytogenetics	IgM MFIR	IgD MFIR
57	I	57	M	U	neg	pos	del11q, del13q	8.49	11.89
58	I	59	M	U	pos	nd	del13q	121.86	55.98
59	I	40	M	U	neg	nd	del13q	51.84	27.08
60	IV	65	M	U	pos	pos	del11q	55.64	34.26
61	0	66	M	U	pos	nd	del11q	10.31	2.86
62	I	62	F	M	neg	neg	neg	14.40	33.10
63	I	67	F	M	neg	nd	del13q	65.13	43.59
64	II	63	M	M	pos	nd	tri12	7.79	4.47
65	I	61	F	M	neg	neg	neg	72.60	93.72
66	0	64	M	M	neg	nd	neg	13.75	60.00
67	0	54	F	U	neg	pos	del13q	71.73	38.17
68	II	68	M	U	neg	pos	tri12	113.29	98.24
69	0	66	M	U	neg	pos	del13q	61.73	42.64
70	I	66	F	U	nd	nd	tri12	57.90	78.08
71	0	67	M	U	neg	neg	neg	35.02	26.39
72	I	63	F	U	neg	pos	del17p	106.88	7.29
73	I	62	M	U	pos	neg	del 11q, del13q	179.83	8.67
74	I	72	M	U	neg	neg	del 11q, del13q	64.40	59.06
75	I	76	F	U	nd	nd	nd	42.55	18.78
76	I	74	F	U	neg	nd	tri12	136.16	54.88
77	II	77	F	U	nd	nd	del13q	143.19	68.98
78	I	54	M	M	neg	neg	del13q	53.58	28.48
79	I	73	M	M	pos	pos	tri 12	28.73	41.83
80	I	60	F	U	neg	neg	del11q, del13q	22.59	33.39
81	I	60	M	U	pos	pos	tri12	78.86	84.12
82	I	58	F	U	neg	pos	del13q	76.67	34.31
83	I	69	M	U	neg	pos	del11q, del17p	57.82	25.21
84	I	66	M	U	pos	nd	del13q	51.12	54.92

Rai stage of disease, age at diagnosis, sex, Immunoglobulin Heavy Chain Variable region (*IGHV*) gene mutational status (M: M-CLL; U: U-CLL), CD38 expression (pos: positive; neg: negative), ZAP70 expression (pos:positive; neg:negative), cytogenetic abnormalities (del: deletion; tri: trisomy; neg: no abnormalities), and mean fluorescent intensity ratios (MFIR) of IgM and IgD BCRs. *IGHV* gene

J Immunol. Author manuscript; available in PMC 2017 September 15.

mutational analysis was performed by PCR followed by direct sequencing and 98% cut-off was used for mutational status assessment. CD38 expression was determined by flow cytometry and 30% positivity was used as cut-off. ZAP70 expression was evaluated by immunohistochemical staining of bone marrow biopsies. Cytogenetic abnormalities were determined by FISH analysis. nd: not determined. IgM and IgD levels were determined by flow cytometry.